Biomaterials Advances 154 (2023) 213623

Contents lists available at ScienceDirect

Biomaterials Advances

journal homepage: www.journals.elsevier.com/materials-science-and-engineering-c

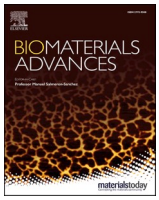

# Development of ibuprofen-loaded electrospun materials suitable for surgical implantation in peripheral nerve injury

Karolina Dziemidowicz [a,b,c,*,1], Simon C. Kellaway [a,b,1], Owein Guillemot-Legris [a,b], Omar Matar [a,b], Rita Pereira Trindade [a,b], Victoria H. Roberton [a,b], Melissa L.D. Rayner [a,b,2], Gareth R. Williams [c,2], James B. Phillips [a,b,2]

[a] Centre for Nerve Engineering, UCL School of Pharmacy, 29-39 Brunswick Square, London WC1N 1AX, United Kingdom of Great Britain and Northern Ireland
[b] Department of Pharmacology, UCL School of Pharmacy, 29-39 Brunswick Square, London WC1N 1AX, United Kingdom of Great Britain and Northern Ireland
[c] Department of Pharmaceutics, UCL School of Pharmacy, 29-39 Brunswick Square, London WC1N 1AX, United Kingdom of Great Britain and Northern Ireland

ARTICLE INFO

*Keywords:*
Electrospinning
Peripheral nerve injury
Implants
Polymer
Biomaterial

ABSTRACT

The development of nerve wraps for use in the repair of peripheral nerves has shown promise over recent years. A pharmacological effect to improve regeneration may be achieved by loading such materials with therapeutic agents, for example ibuprofen, a non-steroidal anti-inflammatory drug with neuroregenerative properties. In this study, four commercially available polymers (polylactic acid (PLA), polycaprolactone (PCL) and two *co*-polymers containing different ratios of PLA to PCL) were used to fabricate ibuprofen-loaded nerve wraps using blend electrospinning. In vitro surgical handling experiments identified a formulation containing a PLA/PCL 70/30 molar ratio *co*-polymer as the most suitable for in vivo implantation. In a rat model, ibuprofen released from electrospun materials significantly improved the rate of axonal growth and sensory recovery over a 21-day recovery period following a sciatic nerve crush. Furthermore, RT-qPCR analysis of nerve segments revealed that the anti-inflammatory and neurotrophic effects of ibuprofen may still be observed 21 days after implantation. This suggests that the formulation developed in this work could have potential to improve nerve regeneration in vivo.

## 1. Introduction

Improving clinical outcomes following peripheral nerve injury (PNI) remains a challenge. Multiple avenues are being explored to overcome this issue, ranging from developing microsurgical techniques [1] to tissue engineering solutions and cell therapies [2,3]. Chronic denervation of muscle causes atrophy [4], whilst prolonged denervation of the distal nerve stump leads to a loss in the potential of Schwann cells to provide a supportive environment for axonal regeneration [5]. Therefore, by accelerating the rate of regeneration, it is possible to improve functional recovery due to a rapid reinnervation of the distal nerve and target organs [6,7]. A range of growth factors and small molecules which could increase regeneration rate following a nerve injury have been identified [8,9]. For instance, the non-steroidal anti-inflammatory drug (NSAID) ibuprofen has shown potential in accelerating nerve regeneration. This is suggested to be through its agonistic action on peroxisome proliferator-activated receptor gamma (PPARγ), resulting in neurite extension as a function of Ras homolog family member A (RhoA) inactivation [10].

While drugs to aid PNI recovery could be administered systemically, this raises a number of challenges in terms of targeting the drug to the injury site, potentially leading to significant and detrimental off-target side effects. These issues can be overcome using drug-loaded biomaterials, which can deliver therapeutics directly to the site of action, minimising side-effects associated with their systemic administration and maximising their efficacy [11].

Drug-loaded synthetic biomaterials can be fabricated using electrospinning. In this approach, a polymer solution is ejected through a

* Corresponding author at: Department of Pharmaceutics, UCL School of Pharmacy, 29-39 Brunswick Square, London WC1N 1AX, United Kingdom of Great Britain and Northern Ireland.
*E-mail address:* k.dziemidowicz@ucl.ac.uk (K. Dziemidowicz).
[1] These authors contributed equally.
[2] Joint senior authors.

https://doi.org/10.1016/j.bioadv.2023.213623
Received 27 March 2023; Received in revised form 28 August 2023; Accepted 8 September 2023
Available online 1 October 2023

charged needle (a spinneret) onto a collector. The electric field maintained between the metal collector and the spinneret facilitates evaporation of the electrospinning solvent, resulting in the formation of fibrous structures with tuneable mechanical and physicochemical properties [12]. A range of pharmaceutical polymers has been explored for the preparation of electrospun nerve repair materials. Polycaprolactone (PCL) and polylactic acid (PLA) as well as poly-lactide-*co*-caprolactone copolymers are perhaps the most commonly used, owing to their slow degradation rate and well-described biocompatibility [13–17] Recently we showed that controlled release of ibuprofen from ethylene vinyl acetate and polylactic-*co*-glycolic acid electrospun wraps can improve functional and histological outcomes in a rat sciatic nerve injury model [18]. Several other drug-loaded electrospun formulations have been explored in animal models of PNI [19–21], but their handling properties have not been reported in detail.

Therefore, the primary aim of this study was to produce a synthetic biomaterial-based nerve wrap that releases ibuprofen in a sustained manner. With emphasis on translation, herein we focus on the fabrication of user-friendly materials that can be easily wrapped around the nerve in a surgical setting. We explored encapsulating ibuprofen sodium in four commercially available polymers to formulate electrospun nerve wraps with appropriate mechanical and drug release properties. The therapeutic effect of ibuprofen eluted from one of the biomaterials was then tested in vivo in a rat sciatic nerve crush model.

## 2. Materials and methods

### 2.1. Experimental materials

Samples of PURASORB 05, PURASORB 7015 and PURASORB 8516 were supplied by Corbion. Poly(ε-caprolactone) (80 kDa), hexafluoro-2-propanol and ibuprofen sodium salt were purchased from Sigma-Aldrich. Neurofilament-H primary antibody was supplied by Eurogentec. DyLight-549 goat anti-mouse secondary antibody was purchased from Vector laboratories.

### 2.2. Electrospinning of ibuprofen formulations

Electrospun fibres were fabricated using a Fluidnatek LE-50 electrospinning instrument (Bioinicia). The polymers were dissolved at 17 % *w/v* in hexafluoro-2-propanol (HFIP) and stirred until complete dissolution of the polymer (approximately 12 h). Ibuprofen sodium salt was added to the polymer solution and stirred for another 60 min to achieve a drug-to-polymer ratio of 1:10 w/w. The drug-polymer solution was then loaded into 3 mL syringes to be ejected through a 0.7 mm inner diameter needle. The experiments were conducted at 25 ± 2 °C and relative humidity 35 ± 10 %. The fibres were collected on baking paper on a mandrel (25 mm in diameter) spinning at 200 rpm at 14 cm distance from the spinneret to the collector. The spinneret was scanning parallel to the collector over a distance of 60 mm at 50 mm/s speed to uniformly distribute the fibre on the mandrel. The full set of experimental details is given in Table 1.

### 2.3. Formulation characterisation

A sample of approximately 0.5 cm × 0.5 cm was cut from each fibre formulation. The samples were mounted onto aluminium stubs (TAAB Laboratories) with carbon-coated adhesive tabs and sputter-coated for 5 min with 20 nm gold (Q150R coater, Quorum) in an argon atmosphere and analysed with a cerium hexaboride thermionic filament scanning electron microscope (Phenom Pro, Thermo) connected to a secondary electron detector. The diameter of the fibres was calculated using the ImageJ J.53 K software [22] with a minimum sample size of 100 fibres, from three SEM images. Tensile mechanical testing was performed using a Bose ElectroForce (3200 Series II, TA Instruments) and WinTest 7 software. Material samples were prepared to be 7 mm × 3 mm and thickness was measured using a Digital Material Thickness Gauge (Fowler Pro-max), then samples were clamped using titanium grips with a gauge length of 3 mm. Samples were subjected to quasi-static tensile testing using a strain rate of 0.17 mm/ s in order to obtain stress-strain relationship data and Young's modulus was calculated from the slope of the ascending linear part of the stress-strain curve.

**Table 1**
Summary of final optimised electrospinning parameters used to produce ibuprofen-loaded materials.

| Formulation name | Polymer composition | Supplier | Voltage (kV) | Flow rate (mL/h) | Volume (mL) |
|---|---|---|---|---|---|
| PLA | PURASORB 05 (poly(DL-lactide)) | Corbion | 7–8 | 0.8 | 1.5 |
| PLA/PCL (85/15) | PURASORB 8516 (85 % L-lactide, 15 % caprolactone copolymer) | Corbion | 10–11 | 1.5 | 1.5 |
| PLA/PCL (70/30) | PURASORB 7015 (70 % L-lactide, 30 % caprolactone copolymer) | Corbion | 9–10 | 0.75 | 1.5 |
| PCL | Polycaprolactone (~80 kDa) | Sigma-Aldrich | 13–14 | 0.8 | 1.5 |

### 2.4. Ibuprofen release study

Approximately 5 mg of each formulation was placed in a 28 mL glass vial and phosphate buffered saline (PBS) was added (1.0 mL, pH 7.4). The samples were then placed in a shaking incubator (Incu-Shake MINI, SciQuip) set to 37 °C and 120 rpm. Aliquots (0.2 mL) were collected from the release medium at predetermined timepoints, and the release medium replenished with the same volume of fresh pre-heated medium. Ibuprofen content was measured using a UV spectrophotometer (SpectraMax M2, Molecular Devices) at a wavelength of 222 nm. Each formulation was tested in triplicate, and the results are presented as mean ± SEM ($n = 3$).

### 2.5. In vitro surgical handling study

Tissue phantoms were prepared from a mixture of porcine skin gelatine (Sigma-Aldrich, at 0.02 g per mL in deionised water) and agar (Fluka BioChemika, at 0.1 g per mL in deionised water). The separate solutions were stirred and heated until the solutions cleared (at about 90 °C). The gelatine and agar were then mixed at a 40 % gelatine to 60 % agar volume ratio and stirred under heat (90 °C) for further 60 min. To create the phantom 4.5 mL of the prepared gels were poured into plastic petri dishes (30 mm in diameter; Fig. S1). A strip of silicone tubing (outer diameter = 7 mm) was placed in the dish to create a groove on the surface of the gel. After the gels set, holes were drilled through the petri dish at each end of the groove, the 7 mm tubing was then removed, and silicone tubing of 1.94 mm outer diameter was threaded through the holes and tied in place. The 1.94 mm diameter silicone tube within the groove on the surface of the gelatine/agar gel mimicked an exposed nerve between muscle planes as encountered during nerve repair surgery (with dimensions similar to a rat sciatic nerve). The tissue phantom was completed by adding 2 drops of Neg-50™ (Richard-Allan Scientific) to mimic the wetness of the in vivo environment.

The handling properties of four electrospun formulations were investigated using a double-blinded user experience study (Fig. S2). The study was conducted in a controlled environment. The electrospun flat sheets were cut into 1 cm × 1 cm pieces and presented to the participants in vials. The average thickness of each sample was measured in triplicate using digital callipers (Fowler Pro-max), and the results are presented as mean ± SEM ($n = 9$). A total of 7 adults with experience in

microsurgery, dissection or nerve wrapping were asked to evaluate the formulations in a 2-part survey (Fig. S3). The first part of the survey focused on general material structure properties, aiming to capture the opinion of the participants about how they would expect the materials to perform during handling in a surgical setting. Participants were instructed to remove the sample from the vial and investigate its mechanical properties by handling with tweezers before completing part 1 of the survey. The second part involved wetting the sample in PBS and attempting to wrap the material around the silicone tubing in the peripheral nerve phantom to mimic the in vivo implantation procedure. After all samples were scored, participants were asked to rank all formulations in order of preference (forced-choice ranking). Keyword panels and comment sections were used to gain qualitative descriptions of the formulations. The time it took for participants to wrap the formulations around the peripheral nerve phantom (implantation time) was measured from video recordings of each study.

### 2.6. Nerve wrap performance in rat sciatic nerve crush model

All experimental procedures involving animals were conducted in accordance with the UK Animals (Scientific Procedures) Act (1986), the European Communities Council Directives (86/609/EEC) and approved by the UCL Animal Welfare and Ethics Review Board. A total of 26 male Wister rats (Charles River) between 225 and 250 g were used for the following experiment (including the pilot shown in Fig. S7). A power analysis was performed using G*Power (version 3) [23] and both experimental groups (ibuprofen-loaded material or blank control material) were calculated to include 8 animals each. A crush control group with no material was also included ($n = 6$). Under anaesthesia the left sciatic nerves were exposed at mid-thigh level and a pair of TAAB type 4 tweezers used to create the crush injury. The tweezers were fully closed on the nerve for 15 s then this was repeated twice more, keeping the tweezers perpendicular to the nerve and rotating them through 45° between each crush application. 10–0 sutures were then used to mark the point of crush before the nerve was wrapped with 1 cm × 1 cm sheets of either blank or ibuprofen loaded fibres (Fig. 1). 4–0 sutures were used to close the muscle tissue and stainless-steel wound clips used to close the skin. All animals received Rimadyl (4 mg/kg, subcutaneous injection) and wounds were treated with veterinary wound powder after closure (Battles, UK). Animals were monitored daily for 21 days and then culled using an overdose of anaesthesia.

### 2.7. Von Frey sensory recovery assessment

Animals were placed on an elevated grid and allowed to adjust to their environment for 5 min. Von Frey filaments (0.008 g – 300 g) were pressed against the centre of the animals' hind paw through the grid. A response was determined by the retraction of the paw following the filament stimulus. The threshold response was recorded by decreasing the stimulus until no response was detected. This process was performed prior to surgery, to record baseline sensation, and repeated every 3 or 4 days following the surgery until the end of the experiment.

### 2.8. Nerve sample preparation

Electrospun nerve wraps were removed, and the repaired nerves excised 6 mm proximal and distal to the crush site, as well as taking a segment from the common peroneal nerve 21 mm distal to the injury site (Fig. S4). These nerve segments were fixed for histology in 4 % paraformaldehyde (PFA) overnight at 4 °C. The remainder of the nerve tissue was immediately snap frozen in liquid nitrogen and stored at −80 °C to be used in qPCR analysis.

### 2.9. RNA extraction and real-time qPCR

Total RNA was extracted using the RNeasy Plus Mini Kit (Qiagen) according to the manufacturer's instructions. cDNA was synthesized using the GoScript Reverse Transcriptase kit (Promega). RT-qPCR was performed with a QuantStudio 3 instrument (Applied Biosystems) and analysed with the QuantStudio Design & Analysis Software (Applied Biosystems). PCR reactions were run using the Power SYBR Green PCR Master Mix (Applied Biosystems). The products were analysed by performing a melting curve at the end of the PCR. Data are normalized to the mRNA expression of 3 reference genes: beta-2 microglobulin (B2m), hypoxanthine phosphoribosyltransferase 1 (HPRT1), and ribosomal protein S18 (RPS18). Primer sequences for qPCR are listed in Table 2. All data are presented as mean ± SEM. Statistical analysis was performed using GraphPad Prism version 9.0. The Kolmogorov-Smirnov test was used to assess the normality of the distribution. A two-tailed unpaired *t*-test or a Mann-Whitney test were used for the RT-qPCR data ($^{*}P < 0.05$ and $^{**}P < 0.01$).

### 2.10. Cryo-sectioning

Fixed nerve samples were removed from the PFA, placed in PBS for 24 h, and then sequentially cryoprotected in 15 % followed by 30 % sucrose, both for 24 h. These samples were then placed in 1:1 *v*/v Neg-50™ (Richard-Allan Scientific) and 30 % sucrose and snap frozen in liquid nitrogen. Transverse sections, 10 μm in thickness, were produced, from regions 5 mm and 21 mm distal to the crush site, using a cryostat (HM525Mx) before placing on glass slides (Superfrost™ Plus, Thermo Fisher Scientific) to undergo immunohistochemistry.

### 2.11. Immunohistochemistry

Nerve cryo-sections were washed in immunostaining buffer (0.3 % Triton-X100 in PBS) for 5 min at room temperature to remove any remaining Neg-50™. A blocking solution was prepared using 10 % horse serum in immunostaining buffer and sections were incubated for 30 min, followed by a primary antibody (1:1000 neurofilament; Eurogentec, 0.3 % Triton X100 and 10 % goat serum in PBS) incubation at 4 °C overnight. The nerve cryo-sections were washed with immunostaining buffer and then incubated with 1:400 DyLight 549 in immunostaining buffer for 45 min at room temperature. The nerve sections were washed in PBS and mounted using VectaShield (Vector Laboratories) before imaging.

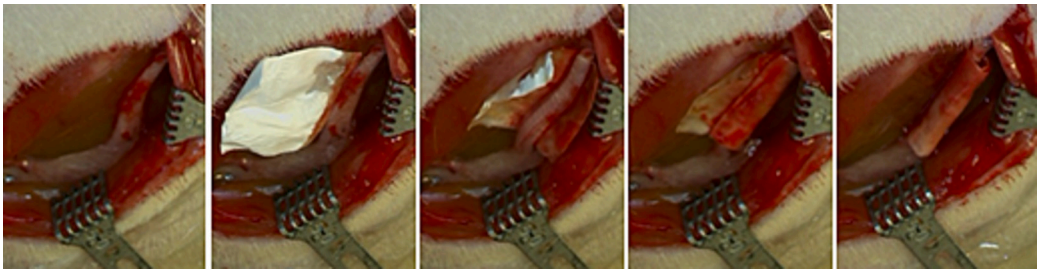

**Fig. 1.** Photographs showing stages of electrospun material implantation procedure in a rat sciatic nerve crush model.

**Table 2**
List of primer sequences used in qPCR experiments.

| Name | Symbol | Forward Primer (5′-3′) | Reverse Primer (5′-3′) |
|---|---|---|---|
| *brain-derived neurotrophic factor* | *Bdnf* | AATGCCGAACTACCCAATC | CATACACAGGAAGTGTCTATCC |
| *beta-2 microglobulin* | *B2m* | CGTGATCTTTCTGGTGCTTG | GGTGGAACTGAGACACGTAG |
| *C-C motif chemokine ligand 2* | *Ccl2* | GCAAGATGATCCCAATGAGTC | GCTTGGTGACAAATACTACAGC |
| *C-C motif chemokine ligand 3* | *Ccl3* | TTTCCTGACCAAGAGAAACCG | AGGCATTTAGTTCCAGCTCAG |
| *Cd68 molecule* | *Cd68* | CCTTTGGATTCAAACAGGAC | GACACATTGTATTCCACTGC |
| *Cd86 molecule* | *Cd86* | ACACGGGCTTGTATGATTG | GAAGTTGGCGATCACTGAG |
| *ciliary neurotrophic factor* | *Cntf* | CAGACCTGACTGCTCTTATGG | TGCTTGCCACTGGTACAC |
| *Glial cell line-derived neurotrophic factor* | *Gdnf* | GCTGACCAGTGACTCCAATATG | TGCCGCCGCTTGTTTATC |
| *hypoxanthine phosphoribosyltransferase 1* | *Hprt1* | ACCTCTCGAAGTGTTGGATAC | GATTCAAATCCCTGAAGTGCTC |
| *interleukin 10* | *Il10* | ACCTGGTAGAAGTGATGCC | GCTGTATCCAGAGGGTCTTC |
| *LIF, interleukin 6 family cytokine* | *Lif* | CAAGAGTCAACTGGCTCAAC | GCATGGAAAGGTGGGAAATC |
| *nerve growth factor* | *Ngf* | GGCATTGACTCCAAGCACTG | CGCCTTGACAAAGGTGTGAG |
| *ribosomal protein S18* | *Rps18* | CTTCGCTATCACTGCCATTAAG | GTGAGGTCAATGTCTGCTTTC |
| *tumor necrosis factor* | *Tnf* | GGCTCCCTCTCATCAGTTC | CGCTTGGTGGTTTGCTAC |

### 2.12. Microscopy and image analysis

Tile scan confocal images were acquired using a Zeiss LSM710 confocal microscope. Neurofilament positive axons were counted from two regions of the nerve, sciatic and common peroneal, using an automated image analysis protocol developed using Volocity™ software (Perkin Elmer).

## 3. Results and discussion

### 3.1. Electrospinning of ibuprofen formulations

A simple method of monoaxial blend electrospinning was selected over more complex setups (such as co-axial electrospinning) to facilitate potential scale-up of the nerve wrap manufacturing process. Commercially available and commonly used pharmaceutical polymers were chosen to accelerate future clinical translation of the formulations. Nanofibres were collected onto a rotating mandrel with the spinneret scanning over a specified distance (6 cm) to ensure uniform distribution of individual fibres and controlled thickness of the overall fibre mat. The formulations were fabricated under controlled environmental conditions (temperature 25 ± 2 °C and relative humidity 35 ± 10 %) to prevent fluctuations in temperature and humidity.

Scanning electron micrographs (Fig. 2A) of the scaffolds revealed successful fabrication of smooth, cylindrical fibres with no visible defects, suggesting appropriate optimisation of electrospinning conditions. All formulations exhibited a unimodal distribution of fibre diameters (Fig. 2B). PCL-based formulations (PLA/PCL 85/15 and 70/30 as well as

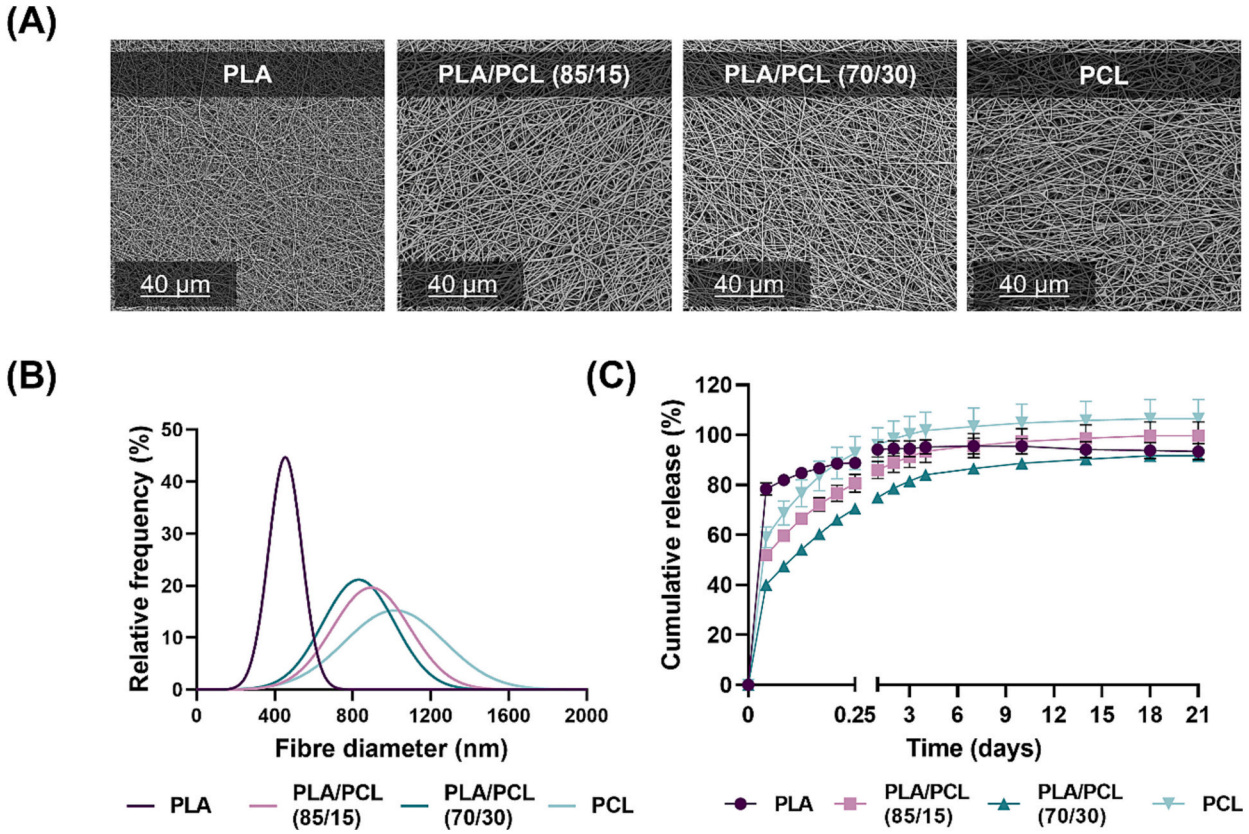


**Fig. 2.** Summary of formulation properties. Scanning electron micrographs (A) reveal cylindrical fibres with no visible defects. A histogram of fibre diameters (B) shows unimodal distribution for all tested formulations. Cumulative ibuprofen release data (C) present an initial burst release followed by a period of sustained release over 21 days (Each formulation was tested in triplicate, and the results are presented as mean ± SEM ($n = 3$)).

PCL) showed mean fibre diameter of 800–1000 nm, while fibres electrospun from PLA exhibited relatively smaller mean diameter of 476 ± 113 nm.

All polymers tested in this study hydrolyse slowly (6+ months) [24–26]. We therefore anticipated ibuprofen to elute from electrospun fibres through diffusion. When following this drug release mechanism, increasing the fibre diameter should lead to prolonged duration of release as the path through which the drug needs to diffuse to reach solution is extended [27]. This indeed was observed in drug release experiments (Fig. 2C), where PLA fibres showed the highest burst release of 78.3 ± 6.5 % within the first hour. The slowest initial release was observed for PLA/PCL (70/30), followed by PLA/PCL (85/15) and PCL. All formulations containing PCL showed a period of sustained release over 21 days.

### 3.2. In vitro surgical handling experiments

Although surface hydrophobicity (Fig. S5A) or mechanical properties, such as Young's modulus (Fig. S5B), of electrospun materials for peripheral nerve injury are typically reported [28,29], the results often do not reflect the overall surgical handling experience. Hence, we developed a survey-based user experience study for screening of nerve-wrapping materials prior to in vivo studies. In an attempt to minimise the use of animals, a fully synthetic tissue phantom was created, aiming to mimic the in vivo environment of a rat sciatic nerve crush model (Fig. S1). A group of participants with prior peripheral nerve microsurgery experience were invited to evaluate four electrospun formulations, reflecting on their general handling properties (such as tearability or stretchability) and ability to wrap around the peripheral nerve phantom (Fig. 3A). Each sample handling test was video recorded (Fig. S6). PLA was described as 'brittle', 'crumbly', 'weak', 'tearable' and 'fragile', while samples containing PCL (PLA/PCL (70/30), PLA/PCL (85/15), PCL) as 'robust', 'pliable' and 'strong'. This correlates positively with previously published studies describing favourable mechanical properties of electrospun PCL scaffolds in tissue engineering applications [30]. The time needed to securely wrap the material around the peripheral nerve phantom was ~50–100 s, and no major differences in wrapping time were observed between formulations (Fig. 3B).

Thickness of electrospun implants is an important parameter as it will affect the mechanical properties of the overall product, influencing its handling and surgical implantability. Although the polymer mass used to fabricate electrospun fibres was uniform for all tested formulations (~290 mg), there were noticeable differences observed in overall electrospun material thickness. The average thickness of PLA, PCL and PLA/PCL (70/30) formulations was 40–60 μm (Fig. 3C), which participants described as 'thin'. On the contrary, fibres prepared from PLA/PCL (85/15) were significantly thicker (140 μm). The higher thickness of PLA/PCL (85/15) was clearly noticed based on the comments provided by participants, who described it as 'thick' and 'with potential to unwrap'.

The participants were also asked to rank the formulations in order of preference (forced-choice preference, no ties allowed [31]), where '1' described most preferred and '6' least preferred. Overall, PLA/PCL 70/30 achieved the highest scores, closely followed by PCL, PLA/PCL 85/15 and PLA. Finally, we asked the participants to summarise their findings by confirming whether they would feel comfortable implanting the tested materials in an in vivo setting (Fig. S7). Once again, PLA/PCL 70/30 was a clear favourite, with ~93 % of positive responses, followed by PCL (~71 %), PLA/PCL 85/15 (~50 %) and PLA (~14 %).

Based on the in vitro surgical handling assessment as well as favourable ibuprofen release profile, PLA/PCL (70/30) was identified as the candidate formulation for further in vivo investigation. A pilot study in a rat sciatic nerve crush model ($n = 2$) aimed to compare the in vitro handling properties of PLA/PCL (70/30) with observations in vivo, as

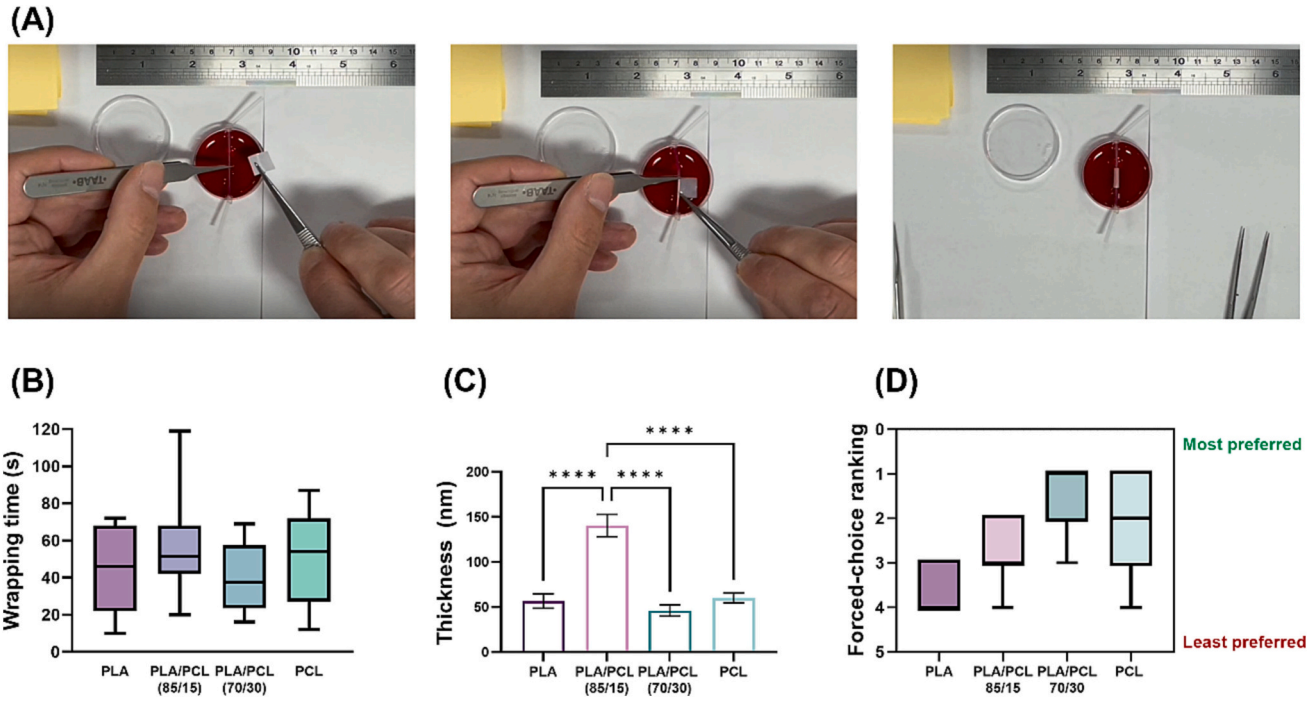


**Fig. 3.** Summary of in vitro surgical handling experiment. Stills from a video recording show different stages of electrospun fibre wrapping around a synthetic nerve phantom (A). The recordings were used to measure time needed to successfully wrap the fibre around silicon tubing mimicking a nerve (B; data presented as mean ± SEM; $n = 7$ (PLA and PCL), n = 7 in duplicate (PLA/PCL 85/15 and PLA/PCL 70/30)). The participants were asked to comment on the overall wrapping properties while handling the material. The differences in material thickness (C; data presented as mean ± SEM, $n = 9$. One-way ANOVA with post hoc Tukeys' multiple comparisons test, $^{****}P < 0.0001$) were reflected in the open-ended answers to the in vitro handling survey. Forced-choice ranking (D; data presented as mean ± SEM, $n = 7$ (PLA and PCL), $n = 14$ (PLA/PCL 85/15 and PLA/PCL 70/30)) identified the formulation most preferred for further in vivo investigation (PLA/PCL 70/30).

well as a macroscopic assessment of fibrosis. Both blank and ibuprofen-loaded formulations (Fig. S8A) wrapped easily around the sciatic nerve (Fig. S8B), which was consistent with the results of the in vitro handling experiment. After 28 days in vivo, no noticeable fibrosis was observed around the implant (Fig. S8C), which remained structurally intact and could be removed from the nerve with ease, suggesting the appropriateness of PLA/PCL (70/30) for nerve-wrapping formulations. The in vivo implantation times (Fig. S8D) were comparable to those measured in the in vitro setting (Fig. 3B), which further supports the suitability of the peripheral nerve phantom for material screening.

### 3.3. Ibuprofen released from electrospun fibres exerts a therapeutic effect

In an attempt to investigate the effect of ibuprofen released from fibres on neuronal growth following injury, a rat sciatic nerve crush model study was performed. In this model, axons distal to the crush site degenerate and then regeneration progresses from the proximal nerve segment back to the target organs in a predictable manner, with restoration of specific functions detectable after 3 weeks, enabling the effect of treatments that modulate regeneration rate to be tested [32]. The animals were culled at 21 days post-surgery and nerve tissue sections assessed 5 mm and 21 mm distal to the injury site. The 21 mm distal location was within the common peroneal branch of the sciatic nerve whereas the 5 mm distal location was proximal to the branch point. Fig. 4 shows examples of histological sections immunostained to detect neurofilament from the 5 mm and 21 mm regions of the nerve (Fig. 4A) and axon counts determined by quantifying sections from all animals (Fig. 4B).

In this study we observed axonal numbers in nerve tissue 5 mm distal to the crush site and also within the deep common peroneal nerve (21 mm distal to the crush site). Whilst no significant difference in axon number was observed within the 5 mm distal region of the sciatic nerve, the 1.3-fold increase of axon number in the ibuprofen group within the 21 mm region was significant ($P = 0.0008$). This is consistent with local ibuprofen delivery accelerating the rate of axonal growth, further supported by the von Frey data (Fig. 4C), which showed a significant difference between treatments ($P = 0.02$), suggesting improved recovery in the ibuprofen group. Systemic ibuprofen delivery over 3 months via osmotic minipumps has previously been shown to increase total axonal area in a tibial nerve injury model [33]. Rayner et al. subsequently demonstrated that ibuprofen increased the rate of neurite growth in vitro [34], and improved regeneration following nerve crush when delivered locally in vivo [18]. The present study provides additional evidence in support of local ibuprofen delivery providing benefit following nerve injury, introducing for the first time an electrospun PLA: PCL (70/30) degradable biomaterial with optimal handling properties.

### 3.4. Molecular effects of ibuprofen persist at 21 days

Previous studies suggested that the positive effect of ibuprofen following nerve injury might be due to it acting as a PPARγ agonist within regenerating neurons [33–35] however this does not take into account the involvement of multiple cell types in addition to neurons, or the ability of ibuprofen to inhibit cyclooxygenase. Therefore, some of the molecular changes in nerve tissue evoked by local delivery of ibuprofen in this study were explored using RT-qPCR analysis. Twenty-one days following crush and administration of ibuprofen-loaded or blank fibres, distal nerve tissue between the 5 and 21 mm regions was analysed in terms of expression changes in genes associated with key anti-inflammatory and neuroregenerative processes (Fig. 5).

At 21 days post-injury, mRNA relative expression of the neurotrophic factors *Ngf* and *Gdnf* was found to be significantly elevated in the ibuprofen-loaded fibre group, showing fold changes in expression of 129.6 ± 5.6 % and 265.4 ± 76.8 % compared with the blank fibre group levels, respectively. Additionally, *Bdnf* and *Lif* mRNA expression was further increased (233.6 ± 62.0 % and 190.4 ± 53.3 %, respectively) in the treatment group, although these differences were not significant. Although NSAIDs have been shown to promote NGF secretion in vitro via COX inhibition [36], their effect on neurotrophic factor upregulation in vivo is not well established. The upregulation in neurotrophic factor expression following nerve injury observed in this study indicates that there may be a growth factor-mediated effect of ibuprofen on neuroregeneration, but this requires further studies to understand the underlying mechanism. Additionally, we observed a statistically significant increase in expression of mRNA for *Il10*, a cytokine commonly associated with an anti-inflammatory response, to 208.0 ± 29.5 % relative to the blank fibre group. Interestingly, expression of the pan-macrophage marker *Cd68* was reduced by 58.4 ± 9.0 % when

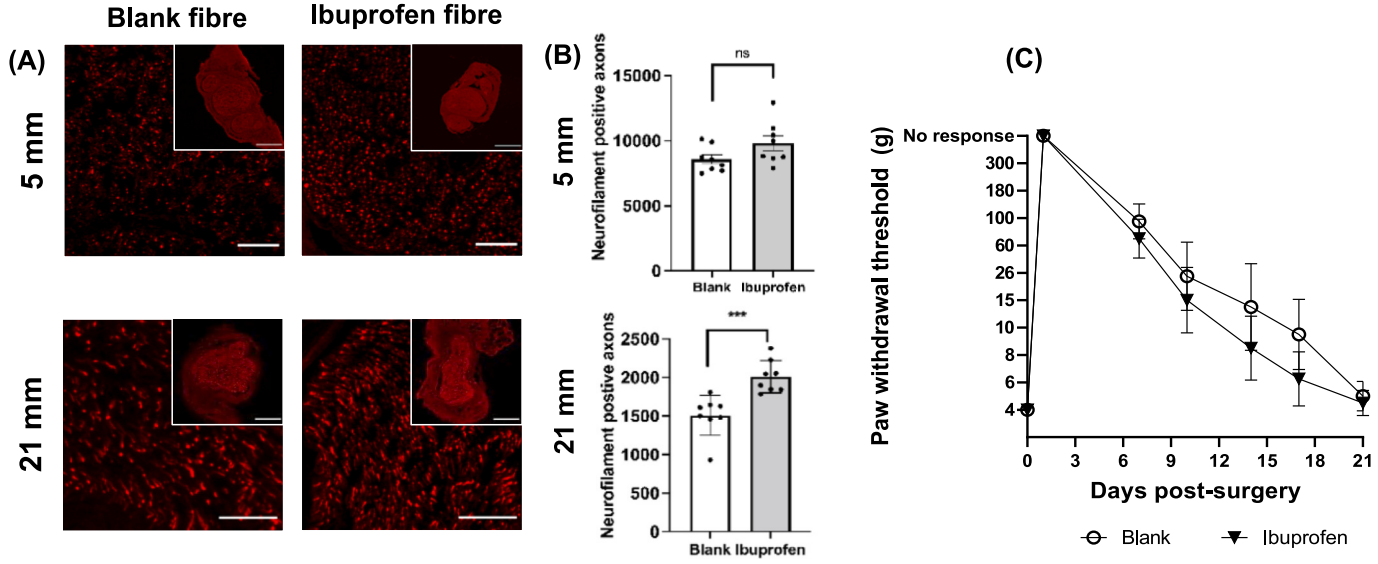


**Fig. 4.** Representative images of nerve sections within the 5 mm and 21 mm distal regions of rat nerves 21 days after sciatic nerve crush injury (A). Axon counts for transverse sections through nerves 5 mm and 21 mm distal to the crush injury site (B). Scale bars = 50 μm, inset scale bars = 500 μm (5 mm) and 200 μm (21 mm). Crush control (no fibre) neurofilament positive axons = 1471 ± 305. All data are presented as mean ± SEM, $n = 8$ (experimental groups), $n = 6$ (crush control). Unpaired *t*-test, $^{***}P < 0.001$. Von Frey sensory measurements for both crush injury groups over the 21-day recovery period (C). Two-way ANOVA showed a significant difference between blank and ibuprofen treatment groups ($P = 0.02$).

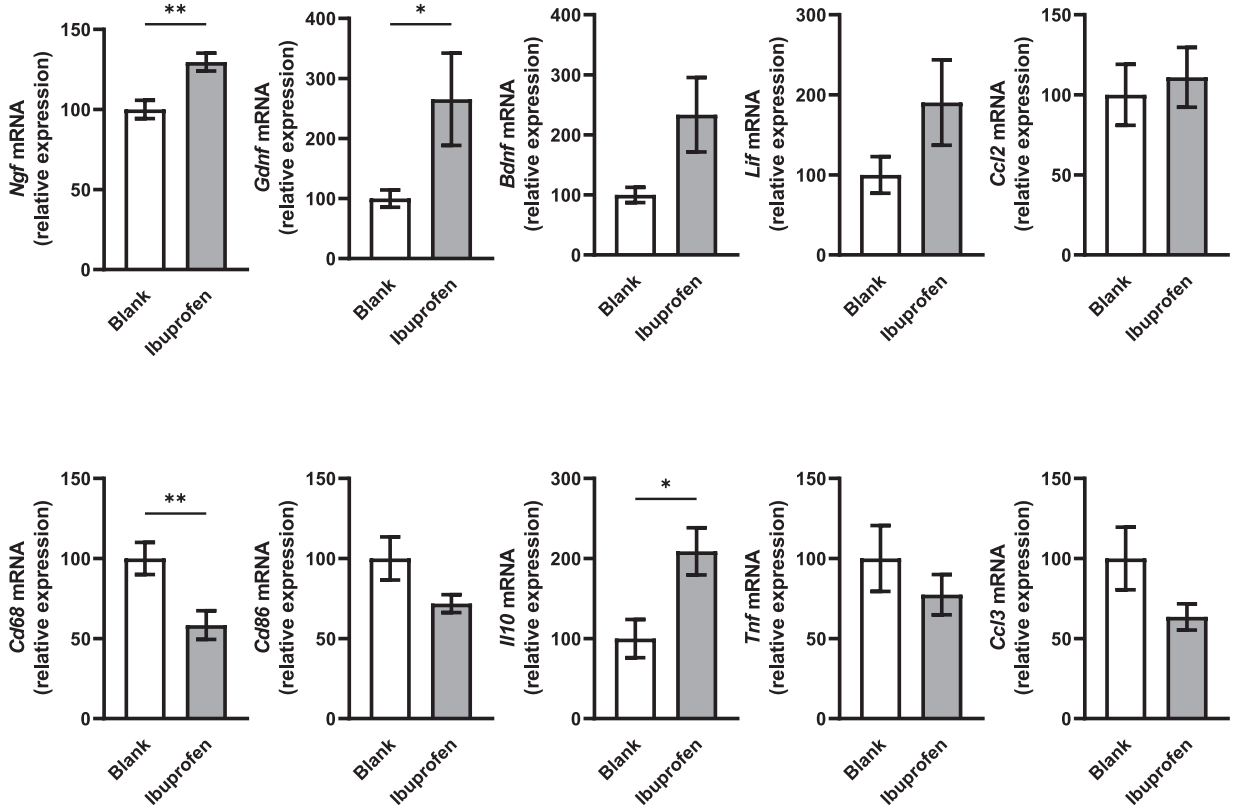


**Fig. 5.** Treatment with ibuprofen-loaded fibres modifies the expression of growth factors and inflammatory markers in the distal sciatic nerve. mRNA relative expression of growth factors, inflammatory markers, and macrophage markers in the distal sciatic nerve 21 days post crush injury. Results are expressed relative to the blank fibre group (Blank) set at 100 %. Data are expressed as mean ± SEM, $n = 8$; Kolmogorov-Smirnov test was used to assess the normality of the distribution; *t*-test or Mann-Whitney test (*$P < 0.05$ and **$P < 0.01$).

compared to the blank fibre group. This has also been reported by Dong et al. (2014) in a neurodegeneration mouse model whereby ibuprofen significantly reduced *Cd68* expression [37]. *Cd86*, *Ccl3*, and *Tnf* all showed modest, though non-significant, reductions in expression in the ibuprofen group compared to the blank fibre. This is consistent with previous studies that show little change in *Tnf* expression when ibuprofen was delivered locally to a tendon injury model [38].

These results suggest that the effects of the drug in nerve tissue are persistent to at least 21 days in vivo. This may be due to the sustained release of ibuprofen resulting in continuous exposure, or a lasting change initiated by the loading dose released from the material. Further studies should explore this phenomenon in order to understand the mechanism by which ibuprofen alters gene expression and regeneration rate in nerve tissue. This in turn could influence future development of biomaterials for local delivery of ibuprofen, optimising formulations to provide controlled release of the drug.

## 4. Conclusion

In this study we successfully created four different electrospun nerve wrap materials loaded with ibuprofen. We further presented an in vitro material handling model, using a synthetic nerve tissue phantom, that proved to be a useful tool for the screening of biomaterial formulations in their ability to be utilised as nerve wraps. Subsequently we used a formulation with appropriate handling properties to deliver ibuprofen to nerves following crush injury in a rat model, resulting in improved outcome measures. Persistent effects of the drug-eluting material were observed at 21 days, in particular the upregulation of neurotrophic factors. Overall, the findings in this study further confirm the beneficial effect of small molecule drug delivery using nerve-wrapping electrospun materials.

## CRediT authorship contribution statement

**Karolina Dziemidowicz**: Conceptualisation, Methodology, Formal analysis, Investigation, Data curation, Writing – original draft, Writing – review and editing, Visualisation. **Simon C Kellaway:** Methodology, Formal analysis, Investigation, Data curation, Writing – original draft, Writing – review and editing, Visualisation. **Owein Guillemot-Legris:** Investigation, Formal analysis, Visualisation, Writing – review and editing. **Gareth Williams:** Conceptualisation, Writing – review and editing, Supervision, Funding acquisition. **Victoria H. Roberton:** Investigation, Methodology, Writing – review and editing. **Omar Matar:** Investigation. **Rita Pereira Trinidade:** Methodology. **Melissa** L. **D. Rayner:** Conceptualisation, Methodology, Investigation, Writing – review and editing, Supervision, Project administration, Funding acquisition. **James B. Phillips:** Conceptualisation, Writing – review and editing, Supervision, Project administration, Funding acquisition.

## Declaration of competing interest

The authors declare that they have no known competing financial interests or personal relationships that could have appeared to influence the work reported in this paper.

## Data availability

Data will be made available on request.

## Acknowledgements

The authors would like to thank Corbion for providing free samples of polymers used in this research. We would also like to thank Dr. David

Gathercole for the confocal microscopy training and technical support, Dr. Isabel Kingston for supporting this project, as well as Dr. Holly Gregory and Dr. Matthew Willcox for their assistance during animal surgeries and participation in the surgical handling study. This work was supported by funding from the 2018 UCL Rosetrees Stoneygate Prize, the EPSRC (EP/R004463/1; EP/L01646X), the UCL Technology Fund and the UCL Therapeutic Acceleration Support scheme supported by funding from MRC Confidence in Concept 2020 (UCL MC/PC/19054).

## Appendix A. Supplementary data

Supplementary data to this article can be found online at https://doi.org/10.1016/j.bioadv.2023.213623.

## References

[1] L. Dvali, S. Mackinnon, The role of microsurgery in nerve repair and nerve grafting, Hand Clin. 23 (2007) 73–81, https://doi.org/10.1016/j.hcl.2007.02.003.
[2] M. Wilcox, H. Gregory, R. Powell, T.J. Quick, J.B. Phillips, Strategies for Peripheral Nerve Repair, Curr Tissue Microenviron Rep, 2020, https://doi.org/10.1007/s43152-020-00002-z.
[3] M. Sarker, S. Naghieh, A.D. McInnes, D.J. Schreyer, X. Chen, Strategic design and fabrication of nerve guidance conduits for peripheral nerve regeneration, Biotechnol. J. 13 (2018) 1–16, https://doi.org/10.1002/biot.201700635.
[4] T.Y. Kostrominova, Skeletal muscle denervation: past, present and future, Int J Mol Sci. 23 (2022), https://doi.org/10.3390/ijms23147489.
[5] S. You, T. Petrov, P.H. Chung, T. Gordon, The expression of the low affinity nerve growth factor receptor in long-term denervated Schwann cells, Glia. 20 (1997) 87–100, https://doi.org/10.1002/(SICI)1098-1136(199706)20:2<87::AID-GLIA1>3.0.CO;2-1.
[6] K. Bergmeister, S. Daeschler, P. Rhodius, P. Schoenle, A. Böcker, U. Kneser, L. Harhaus, Promoting axonal regeneration following nerve surgery: A perspective on ultrasound treatment for nerve injuries, Neural Regen Res. (2018), https://doi.org/10.4103/1673-5374.237113.
[7] T. Gordon, K.M. Chan, O.A.R. Sulaiman, E. Udina, N. Amirjani, T.M. Brushart, Accelerating axon growth to overcome limitations in functional recovery after peripheral nerve injury, Neurosurgery (2009), https://doi.org/10.1227/01.NEU.0000335650.09473.D3.
[8] O. Bota, L. Fodor, The influence of drugs on peripheral nerve regeneration, Drug Metab. Rev. 51 (2019) 266–292, https://doi.org/10.1080/03602532.2019.1632885.
[9] M.L.D. Rayner, J. Healy, J.B. Phillips, Repurposing small molecules to target ppar-γ as new therapies for peripheral nerve injuries, Biomolecules 11 (2021), https://doi.org/10.3390/biom11091301.
[10] J. Dill, A.R. Patel, X.L. Yang, R. Bachoo, C.M. Powell, S. Li, A molecular mechanism for ibuprofen-mediated RhoA inhibition in neurons, Journal of Neuroscience (2010), https://doi.org/10.1523/JNEUROSCI.5045-09.2010.
[11] K. Ye, H. Kuang, Z. You, Y. Morsi, X. Mo, Electrospun nanofibers for tissue engineering with drug loading and release, Pharmaceutics (2019), https://doi.org/10.3390/pharmaceutics11040182.
[12] K. Dziemidowicz, Q. Sang, J. Wu, Z. Zhang, F. Zhou, J.M. Lagaron, X. Mo, G.J. M. Parker, D.-G. Yu, L.-M. Zhu, G.R. Williams, Electrospinning for healthcare: recent advancements, J Mater Chem B. (2021), https://doi.org/10.1039/D0TB02124E.
[13] B. Xia, Y. Lv, Dual-delivery of VEGF and NGF by emulsion electrospun nanofibrous scaffold for peripheral nerve regeneration, Mater. Sci. Eng. C 82 (2018) 253–264, https://doi.org/10.1016/j.msec.2017.08.030.
[14] D. Zhang, W. Yang, C. Wang, H. Zheng, Z. Liu, Z. Chen, C. Gao, Methylcobalamin-loaded PLCL conduits facilitate the peripheral nerve regeneration, Macromol. Biosci. 20 (2020) 1900382, https://doi.org/10.1002/mabi.201900382.
[15] K. Suzuki, H. Tanaka, M. Ebara, K. Uto, H. Matsuoka, S. Nishimoto, K. Okada, T. Murase, H. Yoshikawa, Electrospun nanofiber sheets incorporating methylcobalamin promote nerve regeneration and functional recovery in a rat sciatic nerve crush injury model, Acta Biomater. 53 (2017) 250–259, https://doi.org/10.1016/j.actbio.2017.02.004.
[16] D.R. Nisbet, A.E. Rodda, M.K. Horne, J.S. Forsythe, D.I. Finkelstein, Neurite infiltration and cellular response to electrospun polycaprolactone scaffolds implanted into the brain, Biomaterials. 30 (2009) 4573–4580, https://doi.org/10.1016/j.biomaterials.2009.05.011.
[17] H. Gregory, J.B. Phillips, Materials for peripheral nerve repair constructs: natural proteins or synthetic polymers? Neurochem. Int. 143 (2021) 104953, https://doi.org/10.1016/j.neuint.2020.104953.
[18] M.L.D. Rayner, A. Grillo, G.R. Williams, E. Tawfik, T. Zhang, C. Volitaki, D.Q. M. Craig, J. Healy, J.B. Phillips, Controlled local release of PPARγ agonists from biomaterials to treat peripheral nerve injury, J. Neural Eng. 17 (2020), 046030, https://doi.org/10.1088/1741-2552/aba7cc.
[19] S. Farzamfar, M. Naseri-Nosar, A. Vaez, F. Esmaeilpour, A. Ehterami, H. Sahrapeyma, H. Samadian, A.A. Hamidieh, S. Ghorbani, A. Goodarzi, A. Azimi, M. Salehi, Neural tissue regeneration by a gabapentin-loaded cellulose acetate/gelatin wet-electrospun scaffold, Cellulose. 25 (2018) 1229–1238, https://doi.org/10.1007/s10570-017-1632-z.
[20] S. Miyamura, T. Iwahashi, J. Sayanagi, Y. Hirai, K. Okada, K. Oka, E. Niiyama, K. Uto, M. Ebara, H. Yoshikawa, T. Murase, H. Tanaka, A nanofiber sheet incorporating vitamin B12 promotes nerve regeneration in a rat Neurorrhaphy model, Plast. Reconstr. Surg. Glob. Open 7 (2019), E2538, https://doi.org/10.1097/GOX.0000000000002538.
[21] V.H. Roberton, H.N. Gregory, U. Angkawinitwong, O. Mokrane, A.S. Boyd, R. J. Shipley, G.R. Williams, J.B. Phillips, Local delivery of tacrolimus using electrospun poly-ε-caprolactone nanofibres suppresses the T-cell response to peripheral nerve allografts, J Neural Eng. (2022), https://doi.org/10.1088/1741-2552/acad2a.
[22] C.A. Schneider, W.S. Rasband, K.W. Eliceiri, NIH image to ImageJ: 25 years of image analysis, Nat. Methods 9 (2012) 671–675, https://doi.org/10.1038/nmeth.2089.
[23] F. Faul, E. Erdfelder, A.-G. Lang, A. Buchner, G*power 3: a flexible statistical power analysis program for the social, behavioral, and biomedical sciences, Behav. Res. Methods 39 (2007) 175–191, https://doi.org/10.3758/BF03193146.
[24] M. Zegre, J. Barros, I.A.C. Ribeiro, C. Santos, L.A. Caetano, L. Gonçalves, F. J. Monteiro, M.P. Ferraz, A. Bettencourt, Poly(DL-lactic acid) scaffolds as a bone targeting platform for the co-delivery of antimicrobial agents against *S. aureus*-C. albicans mixed biofilms, Int J Pharm. 622 (2022), https://doi.org/10.1016/j.ijpharm.2022.121832.
[25] N. Ahola, M. Veiranto, J. Rich, A. Efimov, M. Hannula, J. Seppälä, M. Kellomäki, Hydrolytic degradation of composites of poly(L-lactide-co-ε-caprolactone) 70/30 and β-tricalcium phosphate, J. Biomater. Appl. 28 (2012) 529–543, https://doi.org/10.1177/0885328212462258.
[26] Ż. Górecka, E. Choińska, M. Heljak, W. Święszkowski, Long-term in vitro assessment of biodegradable radiopaque composites for fiducial marker fabrication, Int J Mol Sci. 23 (2022), https://doi.org/10.3390/ijms232214363.
[27] G.R. Williams, B.T. Raimi-Abraham, C.J. Luo, Nanofibres in Drug Delivery, UCL Press, 2018 http://www.jstor.org/stable/j.ctv550dd1.
[28] A.R. D'Amato, D.L. Puhl, S.A.T. Ellman, B. Balouch, R.J. Gilbert, E.F. Palermo, Vastly extended drug release from poly(pro-17β-estradiol) materials facilitates in vitro neurotrophism and neuroprotection, Nat. Commun. 10 (2019) 4830, https://doi.org/10.1038/s41467-019-12835-w.
[29] C. Liu, C. Wang, Q. Zhao, X. Li, F. Xu, X. Yao, M. Wang, Incorporation and release of dual growth factors for nerve tissue engineering using nanofibrous bicomponent scaffolds, Biomed. Mater. 13 (2018) 44107, https://doi.org/10.1088/1748-605X/aab693.
[30] D. Mondal, M. Griffith, S.S. Venkatraman, Polycaprolactone-based biomaterials for tissue engineering and drug delivery: current scenario and challenges, Int. J. Polym. Mater. Polym. Biomater. 65 (2016) 255–265, https://doi.org/10.1080/00914037.2015.1103241.
[31] K. Dziemidowicz, F.L. Lopez, B.J. Bowles, A.J. Edwards, T.B. Ernest, M. Orlu, C. Tuleu, Co-processed excipients for dispersible tablets—part 2: patient acceptability, AAPS PharmSciTech 19 (2018) 2646–2657, https://doi.org/10.1208/s12249-018-1104-2.
[32] G.Q. Gong, B. Bilanges, B. Allsop, G.R. Masson, V. Roberton, T. Askwith, S. Oxenford, R.R. Madsen, S.E. Conduit, D. Bellini, M. Fitzek, M. Collier, O. Najam, Z. He, B. Wahab, S.H. McLaughlin, A.W.E. Chan, I. Feierberg, A. Madin, D. Morelli, A. Bhamra, V. Vinciauskaite, K.E. Anderson, S. Surinova, N. Pinotsis, E. Lopez-Guadamillas, M. Wilcox, A. Hooper, C. Patel, M.A. Whitehead, T.D. Bunney, L. R. Stephens, P.T. Hawkins, M. Katan, D.M. Yellon, S.M. Davidson, D.M. Smith, J. B. Phillips, R. Angell, R.L. Williams, B. Vanhaesebroeck, A small-molecule PI3Kα activator for cardioprotection and neuroregeneration, Nature 618 (2023) 159–168, https://doi.org/10.1038/s41586-023-05972-2.
[33] T. Madura, K. Tomita, G. Terenghi, Ibuprofen improves functional outcome after axotomy and immediate repair in the peripheral nervous system, Journal of Plastic, Reconstructive & Aesthetic Surgery 64 (2011) 1641–1646, https://doi.org/10.1016/j.bjps.2011.07.014.
[34] M.L.D. Rayner, S. Laranjeira, R.E. Evans, R.J. Shipley, J. Healy, J.B. Phillips, Developing an in vitro model to screen drugs for nerve regeneration, Anat. Rec. 301 (2018) 1628–1637, https://doi.org/10.1002/ar.23918.
[35] M.L.D. Rayner, S.C. Kellaway, I. Kingston, O. Guillemot-Legris, H. Gregory, J. Healy, J.B. Phillips, Exploring the nerve regenerative capacity of compounds with differing affinity for PPARγ in vitro and in vivo, Cells. 12 (2022) 42, https://doi.org/10.3390/cells12010042.
[36] W. Alimasi, Y. Sawaji, K. Endo, M. Yorifuji, H. Suzuki, T. Kosaka, T. Shishido, K. Yamamoto, Regulation of nerve growth factor by anti-inflammatory drugs, a steroid, and a selective cyclooxygenase 2 inhibitor in human intervertebral disc cells stimulated with interleukin-1, Spine (Phila Pa 1976) 38 (2013) 1466–1472, https://doi.org/10.1097/BRS.0b013e318294edb1.
[37] Z. Dong, L. Yan, G. Huang, L. Zhang, B. Mei, B. Meng, Ibuprofen partially attenuates neurodegenerative symptoms in presenilin conditional double-knockout mice, Neuroscience (2014), https://doi.org/10.1016/j.neuroscience.2014.03.048.
[38] B.L. Taylor, D.H. Kim, J. Huegel, H.A. Raja, S.J. Burkholder, S.N. Weiss, C.A. Nuss, L.J. Soslowsky, R.L. Mauck, A.F. Kuntz, J. Bernstein, Localized delivery of ibuprofen via a bilayer delivery system (BiLDS) for supraspinatus tendon healing in a rat model, Journal of Orthopaedic Research (2020), https://doi.org/10.1002/jor.24670.